Physics laboratory course

VESPA

An experiment for plasma physics

Emilio Martines, Matteo Zuin

Academic year 2017-2018

Introductoin

The present pages are to be considered a guide to the basic comprhension and the use of a plasma physics experiment, named VESPA ("Vaso per Esperimenti Su Plasmi ed Altro"), operating at the Physics Department of the University of Padova.

The device is made to form a plasma inside a discharge chamber, to perform a characterization of its behaviour in a range of parameters including the plasma current and the neutral gas pressure. The fundamental plasma parameters (density, temperature and electrostatic potential) can be measured ny means of Langmuir probes.

The aim of the experiment is to introduce the student to the experimental plasma physics and to give him the basic knowledge about vacuum systems.

The material in organized as follows:

Chapter 1 In this chapter the basic theoretical concepts necessary to understand the experiment behaviour and to analyze the data are given. In particular, the thermoionic emission phenomenon is introduced, along with the plane diode model (useful for a comprehension of the space charge current limit phenomenon), the Debye sheath concept, the Langmuir probe theory, the ion sound wave basics. Finally, a simplified model of the VESPA experiment is presented.

Chapter 2 Brief introduction to vacuum technology and to diagnostics vacuum systems used in the experiment.

Chapter 3 Description of the experimental device: vacuum system, electric scheme, permanent magnets system.

CHAPTER 1

Basic theory

1.1 What a plasma is

A plasma is defined as a gas which is totally or partially ionized, whose density is sufficiently high to induce collective behaviour. The second part of the definition will not be investigated here in detail: it will be sufficient to know that it is verified in almost all conditions found in the laboratory and in Nature.

The state of plasma, which can be considered as the fourth state of matter, relatively not so frequent on Earth (flames and lightnings are examples of spontaneous plasmas), is instead the most common in the Universe. Indeed, matter can be found in the state of plasma on a wide range of conditions in terms of density and temperature, as shown in Fig. 1.1, where few examples of natural and laboratory plasmas are presented. It is worth to note that in plasma physics density is given as particles per unit volume (usually m^{-3}), while for the temperature the electronvolt (eV) is used. Indeed, temperature is interpreted in terms of mean energy: temperature in eV is obtained from the real temperature (in K) by multiplying by the Boltzmann constant and dividing by the elementary charge e. It is useful to mention that 1 eV corresponds to a temperature of 11600 K.

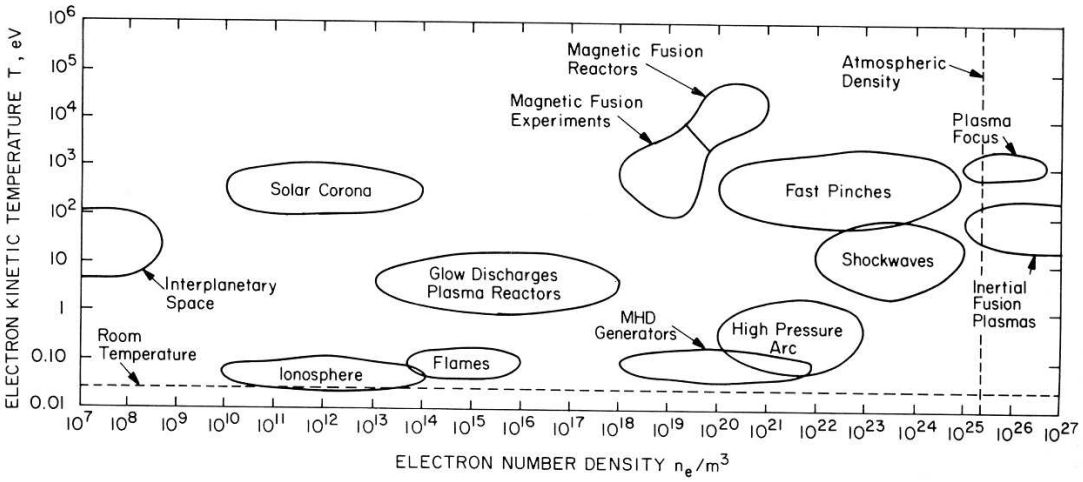

Figure 1.1: *Location of various plasmas in the density-temperature plane. Horizontal and vertical dashed lines indicate the density and the temperature for an atmospheric pressure gas at room temperature.*

The study of laboratory plasmas has received a strong drive from the '50s, when the research on magnetically confined plasmas for thermonuclear fusion application started, with the aim of

realizing the fusion reactions in Deuterium-Tritium plasmas, confined by strong magnetic field in toroidal devices. A further drive came in the '80s from the growth of plasma technologies for thin-film deposition and surface treatment for microelectronic and various industrial purposes.

1.2 How to create a plasma in the laboratory

The most frequently used, but not unique, method to create a plasma in the laboratory is based on the application of electric fields (constant in time or oscillating) to a neutral gas. Such neutral gas must preferentially be at low pressure, as such a condition is favorable for the plasma formation (it must be added that, recently, techniques to get a plasma state at ambient pressure have been successfully developed). The application of an electric field accelerates the free electrons initially present in the gas, which, colliding with the atoms of the gas, induce their ionization.

The process above described finds its simplest application in the case a constant, in time, electric field is applied between two electrodes located in a tube filled with a low-pressure gas. For low voltages the current level is extremely low, mainly driven by the free electrons present in the gas as the result of natural radioactivity and cosmic rays induced ionization. As the voltage is raised, such free electrons can gain enough energy to induce ionization of the gas atoms, thus generating further free electrons, which, if the voltage is sufficiently high, can induce more and more free charges. A voltage known as *break-down* voltage is then reached at which an avalanche phenomenon generates a plasma. The value of such *break-down* voltage, is, in the most favorable conditions (at a gas pressure around 0.1 mbar and for an inter-electrodes distance of 10 cm), around 360V in air and 265V in Argon.

An alternative method to produce a plasma consists in heating the negatively polarized electrode up to extremely high temperatures. This is usually obtained by using a tungsten thin wire carrying a rather high electric current (5-10 A for a 0.1-0.3 mm diameter of the wire). In this case, the thermoionic emission phenomenon is associated to the release from the cathode of an electron current. The generated free electrons are then accelerated towards the anode. The presence in the gas of a number of free electrons much higher than that usually encountered in normal conditions makes the transition to a plasma state no more a real breakdown, but rather a smoother plasma generation at voltages sensibly lower than those needed with the use of a cold cathode (typically of the order of few tens of Volts. This is the method in which the VESPA experiment is operated.

1.3 Thermoionic emission

As said above, the cathode used in the experiment is made of a Tungsten wire which is heated up to very high temperatures (of the order of 2500 K), through an electric current (Ohmic heating). The thermoionic emission phenomenon occurring at such high temperatures is described by Richardson's law, summarized by the formula:

$$\boxed{J = AT^2 \exp\left(-\frac{e\Phi}{kT}\right)} \tag{1.1}$$

in such an expression, J is the electron current density due to the thermoionic emission, Φ is the extraction potential, i.e. the minimum energy to be given to an electron in a metal to make it escape from the metal itself, e is the elementary charge, k is the Boltzmann constant, T is the filament temperature (in Kelvin) and A is a constant depending on the used material. The value of A for Tungsten is 7×10^5 A/m^{2}K^2, while Φ is equal to 4.55 V. A graph of J as a function of T for Tungsten is shown in figure 1.2. It can be seen that as T increases the emitted current also increases very rapidly.

Let us now consider a filament, where a current I_F is driven by a potential difference V_F applied to its extremals (as will be done in the VESPA experiment). The relation between I_F and V_F will be given, following Ohm's law, by the filament resistance, which will be a function of the temperature

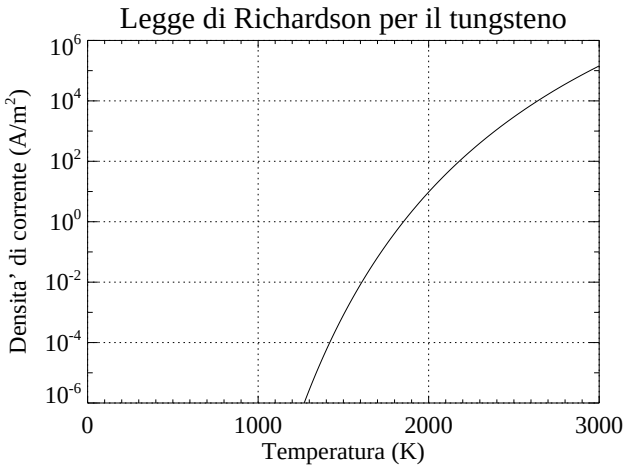

Figure 1.2: *Current density emitted from a Tungsten wire as a function of the temperature.*

(resistivity in a conductor is an increasing function of the temperature). To get information about the temperature, it is possible to write down a second equation which comes from the balance between the Ohmic input power heating the filament and the radiated power from the filament itself (neglecting thermal conduction losses). We thus get for a filament of length L and radius r,

A^10/7 L I^(13/7)
V = --
pi^(13/7) r^(23/7) (2 epsilon alpha)^(3/7)

$$V_F = \rho(T)\frac{L}{\pi r^2} I_F \tag{1.2}$$

$$V_F I_F = \epsilon \alpha T^4 2\pi r L \tag{1.3}$$

In the first equation, Ohm's law, we find the Tungsten resistivity, whose values as a function of T are given in the literature. A fit of such values gives the expression:

$$\rho(T) = \frac{A}{6.2 \times 10^{-11} T^{1.2}} \text{ A m} \qquad (T \text{ in K}). \tag{1.4}$$

Ohm

In the second equation a black body emission has been considered, proportional to T^4, multiplied by an effective emissivity ε taking into account that the Tungsten wire is not a real black body; for Tungsten its value is around 0.3. The Stefan-Boltzmann constant is $\alpha = 5.64 \times 10^{-8}$ J/m^2 K^4. For surface, the lateral surface of the cylinder has been used.

By using these two equations and making the temperature to explicitly disappear, it is possible to evaluate the voltage-current characteristics of the filament. Finally, using the two equations to get the temperature as a function of the current, it is possible through Richardson's law to get the electron emitted current as a function of the current flowing in the filament itself. An example of such calculations, for a 10cm long filament and for three values of its diameter, is shown in fig. 1.3.

1.4 The plane diode model

Before studying the problem of how a Tungsten wire can be used to create plasma, it is useful to consider the simplified problem of the behaviour of electrons when emitted in vacuum. The electron current effectively emitted from a Tungsten wire in vacuum can be lower than that predicted by Richardson's law, because the emitted electrons tend to form a negatively charged cloud around the filament, which, through electrostatic repulsion, impedes the emission of further electrons.

In order to quantify this phenomenon, let's consider a system as that shown in fig. 1.4a. In such a system a cathode emits electrons, with initial velocity v_0, which are accelerated towards the anode located a distance d by means of a potential difference V_0 applied to the electrodes.

If the electrodes surface is very large, it is possible to consider a mono-dimensional model, where all the quantities depend only on the x coordinate. The charge conservation law makes the current

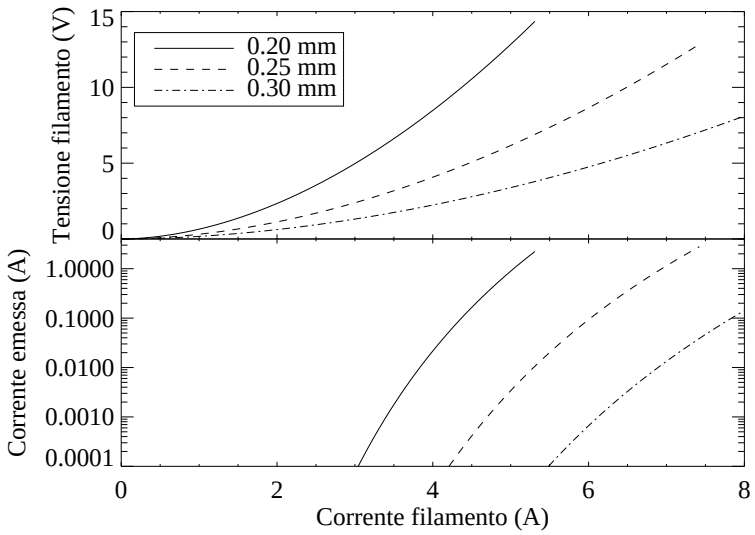

Figure 1.3: *Voltage applied to the filament and emitted electron current as a function of the current flowing in the filament. The three curves correspond to three different values of the filament diameter (10 cm long).*

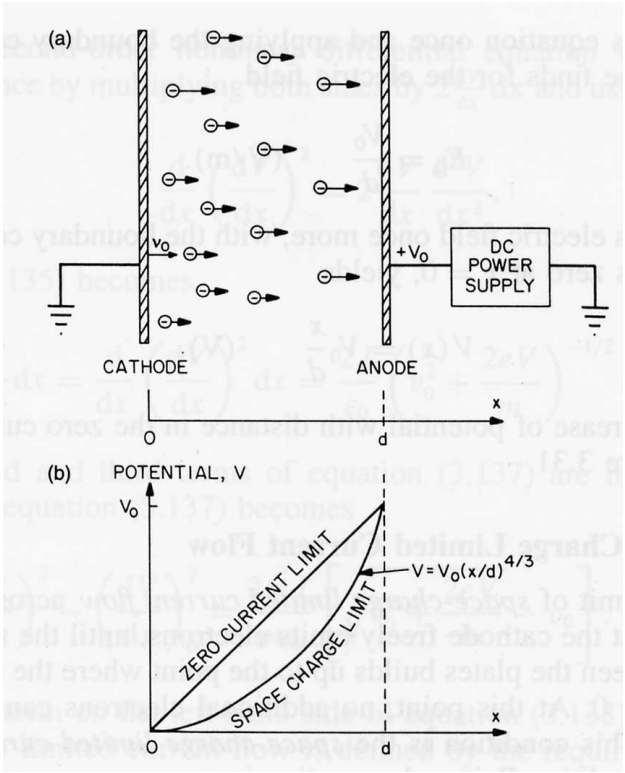

Figure 1.4: *Plane diode scheme (a) and electrostatic potential profile (b).*

density not to depend on x, i.e. $j = env$ is constant (n being the electron density and v the electron velocity).

Let us initially consider the limit of very low current density and hence of very low charge density. In such a case, Poisson equation, allowing evaluating the electrostatic potential in between the two electrodes, reduces to Laplace equation:

$$\frac{d^2V}{dx^2} = -\frac{en}{\varepsilon_0} \approx 0 \tag{1.5}$$

By integrating this equation and applying the boundary conditions $V = 0$ at the cathode ($x = 0$)

and $V = V_0$ at the anode ($x = d$), the voltage linearly increases with x, i.e.

$$V(x) = V_0 \frac{x}{d} \tag{1.6}$$

Let's now include the effect of a finite current density. In this case, it is necessary to evaluate the electron velocity. Applying the energy conservation law, we get

$$\frac{1}{2}mv^2 - eV = \frac{1}{2}mv_0^2 \tag{1.7}$$

da cui

$$v(x) = \sqrt{v_0^2 + \frac{2eV}{m}} \tag{1.8}$$

Poisson equation can thus be rewritten as

$$\frac{d^2V}{dx^2} = -\frac{en}{\varepsilon_0} = \frac{j}{\varepsilon_0 v(x)} = \frac{j}{\varepsilon_0}\left(v_0^2 + \frac{2eV(x)}{m}\right)^{-1/2} \tag{1.9}$$

This 2nd order non-linear differential equation can be once integrated by multiplying both members by $2dV/dx$ and using the identity

$$\frac{d}{dx}\left(\frac{dV}{dx}\right)^2 = 2\frac{dV}{dx}\frac{d^2V}{dx^2} \tag{1.10}$$

We get

$$\left(\frac{dV}{dx}\right)^2 - \left(\frac{dV}{dx}\right)_0^2 = \frac{2mj}{e\varepsilon_0}\left[\sqrt{v_0^2 + \frac{2eV}{m}} - v_0\right] \tag{1.11}$$

At this point, we make use of the so-called "space charge limited current condition" hypothesis, which prescribes that the current emitted from the cathode can grow up to the level that the repulsion from the electron cloud opposes the further emission of electrons, and that this situation arises when the electric field at the cathode is null.

This hypothesis determines the second term in the first member of the equation to be equal to zero.

The obtained equation is not analytically integrable. Nevertheless, by using the hypothesis (usually valid in realistic conditions) that $v_0 \approx 0$, we get the following equation:

$$\frac{dV}{dx} = \sqrt{\frac{2j}{\varepsilon_0}}\left(\frac{2m}{e}\right)^{1/4} V^{1/4}. \tag{1.12}$$

This equation can be integrated, with the condition $V = 0$ at $x = 0$, and we get the following space distribution for the electrostatic potential:

$$\boxed{V(x) = \left(\frac{9j}{4\varepsilon_0}\right)^{2/3}\left(\frac{m}{2e}\right)^{1/3} x^{4/3}.} \tag{1.13}$$

The behaviour of this curve is shown in fig.1.4b, along with that previously found for the limit of very low current density.

Rewriting this relation, so that the current density appears at the first member and evaluating it at $x = d$, Child's law is obtained for a situation with space-charge limited current:

$$\boxed{j = \chi\frac{V_0^{3/2}}{d^2}} \tag{1.14}$$

where

$$\chi = \frac{4\varepsilon_0}{9}\sqrt{\frac{2e}{m}} = 2.334 \times 10^{-6}\mathrm{A/V^{3/2}}. \tag{1.15}$$

Child's law defines the voltage-current characteristics for the plane diode.

At this point, it is important to note that in the plane-diode approach the hypothesis has been implicitly considered that no limit exists in the ability of the cathode to emit electrons, so that space charge current limitation can be satisfied.

In reality, it is well known that a limit indeed exists, given by Richardson's law. As a consequence, in an experimental device operating with a hot cathode, the electric voltage-current characteristics will be made of two parts: for current values low enough the $V_0^{3/2}$ dependence predicted by Child's law will be found; as the voltage is increased, a current saturation will be encountered due to the limit associated to Richardson's law. For the first part of the characteristics, named S zone, we speak of current limited by space charge effects, for the second, named T zone, of current limited by temperature effects. An example of such characteristics is shown in fig.1.5 for three values of the cathode temperature.

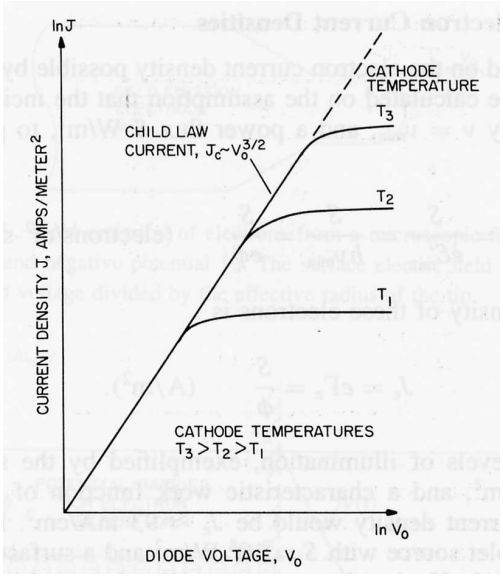

Figure 1.5: *Electric voltage-current characteristics for the plane diode at three different cathode temperatures.*

1.5 Debye sheath theory

An important subject of plasma physics is the Debye sheath. This is a thin sheath of positive charge density which forms around a conducting object immersed in a plasma and kept electrically insulated (floating). The origin of the Debye sheath can be intuitively understood if the higher electron thermal velocity compared to the ion thermal one is taken into account. Electrons are, indeed, usually much faster than ions, not only because they are characterized by higher temperature, but mainly because they have a much lower mass. As a consequence, when an object is immersed in a plasma, it is normally reached by an electron flux much larger than the ion flux. If the object is electrically floating, it rapidly becomes negatively charged. The process continues until such negative charge is large enough to repel electrons and to attract ions, so that the two fluxes become equal. The Debye sheath has thus the effect of shielding the potential of the object, so that the potential difference between it and the plasma is confined in a very short range, of the order of few Debye lengths. The Debye length is defined as:

$$\lambda_d = \sqrt{\frac{\varepsilon_0 k T_e}{e^2 n}} \tag{1.16}$$

where T_e is the electron temperature and n is the density, which in a neutral plasma is the same for ion and electrons (such condition is known as quasineutrality). Typically, in laboratory plasmas,

the Debye length is of the order of 10-100 μm.

It is possible to show that ions are accelerated towards the Debye sheath up to an average velocity, which is equal to

$$c_s = \sqrt{\frac{kT_e}{M}} \tag{1.17}$$

This velocity is known as ion-sound velocity, as it corresponds to propagation velocity of sound waves in a plasma, as will be recalled later. It is worth to note that the temperature at the numerator is the electron temperature (cold ions are considered), while M is the ion mass. As a consequence, the ion flux reaching the object will be

$$\Gamma_i = \frac{1}{2} n c_s \tag{1.18}$$

where the 1/2 factor is due to the acceleration process up to the c_s velocity, which halves the density.

The electrons, in their motion towards the object, feel a retarding electric field. In the hypothesis of maxwellian velocity distribution function, the electron flux to the object will be

$$\Gamma_e = \frac{1}{4} n v_{te} \exp\left(\frac{e(V - V_p)}{kT_e}\right) \tag{1.19}$$

where V is the object potential, V_p is the plasma potential away from the object itself, and v_{te} is the electron thermal velocity, given by

$$v_{te} = \sqrt{\frac{8kT_e}{\pi m}}. \tag{1.20}$$

When the object is electrically insulated, its potential, known as floating potential V_f, can be deduced by the equality$\Gamma_e = \Gamma_i$. One gets

$$\frac{e(V_f - V_p)}{kT_e} = \frac{1}{2} \log\left(\frac{\pi m}{2M}\right) \tag{1.21}$$

which means

$$\boxed{V_f = V_p + \alpha kT_e/e} \tag{1.22}$$

where

$$\alpha = \frac{1}{2} \log\left(\frac{\pi m}{2M}\right) \tag{1.23}$$

in the case of an Argon plasma $\alpha = -5.4$.

The Debye sheath forms even if the object is not floating, but kept at a given potential lower than the plasma potential, by means of a power supply.

1.6 The Langmuir probe

Before defining the model for the VESPA experiment, it is useful to introduce, by means of the concepts above given, the simplest possible diagnostics for plasmas which are not too hot, the Langmuir probe.

A Langmuir probe is mainly a small electrode immersed in the plasma under study. From the electric characteristics of a Langmuir probe it is possible to get information about the electron temperature and density, as well as about the plasma potential. The insertion of an object in a plasma has, necessarily, a perturbing effect, so that, when extremely accurate measurements are needed, special non-invasive techniques must be adopted. On the other hand, the Langmuir probe remains nowadays the most used plasma diagnostics systems, thanks to its simplicity and reliability.

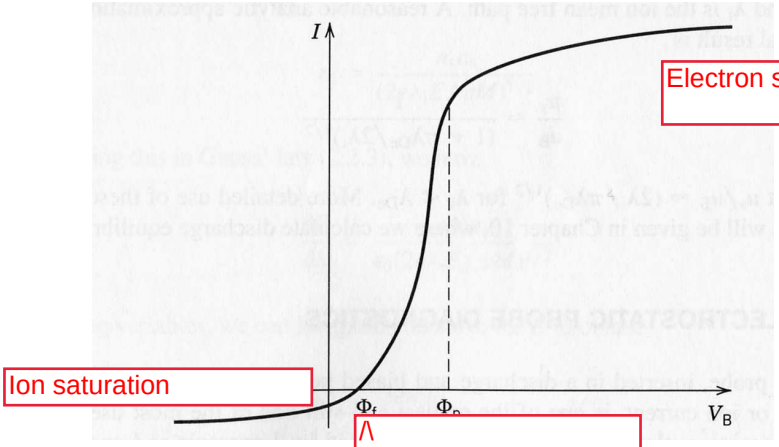

Figure 1.6: *Electrical voltage-current characteristics of a Langmuir probe.*

A schematic Langmuir probe characteristics is shown in figure 1.6. one of the two saturation levels of the current corresponds to the case in which the applied potential is so negative to repel all electrons (ion saturation current); the second corresponds to the opposite limit, when the applied voltage is so positive that all the ions are repelled (electron saturation current). The intersection of the curve with the horizontal axis indicates the situation with null current, and hence it refers to the floating potential.

In order to get an analytic expression of the Langmuir characteristics, at least for applied potential lower than the plasma potential, we can make use of the electron and ion fluxes, given in the previous section.

For a probe area A, the electron current flowing from the probe to the plasma will be given by the expression:

$$I = eA\left[\frac{1}{4}n\sqrt{\frac{8kT_e}{\pi m}}\exp\left(\frac{e(V-V_p)}{kT_e}\right) - \frac{1}{2}n\sqrt{\frac{kT_e}{M}}\right] \tag{1.24}$$

Using the expression found above for the floating potential, such a relation can be rewritten as

$$\boxed{I = I_{si}\left[\exp\left(\frac{e(V-V_f)}{kT_e}\right) - 1\right]} \tag{1.25}$$

where I_{si} is the ion saturation current

$$I_{si} = \frac{1}{2}Aenc_s \tag{1.26}$$

Therefore, a fit of the portion of the characteristics including the ion saturation current and the exponential growth obtained from this formula, gives the three parameters I_{si}, V_f and T_e. From the expression for I_{si} and V_f it is then possible to deduce the density n and the plasma potential V_p.

The part of the electric characteristics associated to the electron saturation region is not used in this procedure. Nonetheless, for plasmas with very low density, and hence very low ion saturation current, the electron saturation current can be used for density evaluation, through the formula

$$I_{se} = \frac{1}{4}Aenv_{te}. \tag{1.27}$$

It is worth to note that the electron saturation current is larger than the ion saturation current by a a factor $(2M/\pi m)^{1/2}$, which for Argon is 216.

In many laboratory situations the experimental characteristics do not necessarily resemble the theoretical (ideal) one. This is because, due to the the gradual expansion of the Debye sheath, which induces the increase of the effective collecting probe area, the ion and electron currents do

not exhibit a clear saturation level. A technique is thus adopted to take into account (and correct) such effect, which will be here described. Such procedure must be used also when analysing the electric characteristics deduced from the Lanmguir probes used in the VESPA experiment.

The procedure is the following (see also figure 1.7):

1. Use a linear fit of the ion saturation current (negative voltages). Such fit must be adopted for voltage levels lower than a certain value, chosen so that the trend is sufficiently linear. The obtained straight line is associated to the ion contribution to the total current by the probe.
2. Subtract from the total current the straight line previously obtained, so that the current driven by the electrons is deduced.
3. The electron current, previously obtained, must be plotted on a logarithmic scale.
4. As shown in figure 1.7), two linear fits, for the two portions of the curve, corresponding to the exponential growth and the saturation part, respectively, must be obtained (indicated in the figure as *bulk electrons* and *saturation region*.
5. The interception of these two fitting lines represents the plasma potential, and the associated current level can be considered as the electron saturation current. From the latter the plasma density can be deduced from the expression (1.27). The slope of the left hand side fit gives the electron temperature, taking into account that the fit is associated to a trend like $\exp(eV/kT_e)$.

It must be noted that the fit, whose slope gives the electron temperature, can, indeed, exhibit two different slopes (indicated in the figure 1.7 as *bulk electrons* and *tail electrons*). This effect is present when the plasma is characterized by an electron velocity distribution resulting as the sum of two maxwellian populations at different temperatures. In this case, the electron temperature to be considered is the colder one, which is also the most populated, associated to the slope of the fit on the right hand side (corresponding to more positive voltage levels).

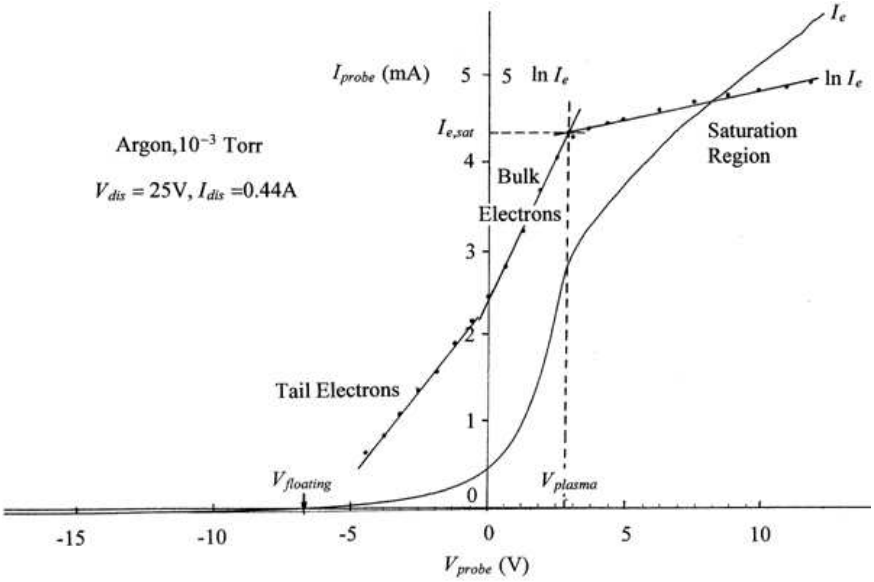

Figure 1.7: *Voltage-current characteristics from a Langmuir probe exhibiting no saturation of the ion and electron currents.*

Ion acoustic waves

1.7 Ion acoustic waves

Sound (acoustic) waves are periodic oscillations of pressure and density. In a neutral gas, these longitudinal waves propagate through binary collisions. When reducing the neutral gas

pressure to the mPa range, ordinary sound waves do no longer propagate due to the long mean free path length. In a plasma, however, sound waves can propagate through the long-range Coulomb interactions of the charged particles. In the low frequency regime (low compared to the so-called ion plasma frequency), ions and electrons oscillate in phase and the corresponding periodic density perturbations are called ion acoustic waves (IAWs). They were first described in 1929 by Tonks and Langmuir. Today, they still play a role in plasma physics as a reliable diagnostics tool, in particular in multi-ion component plasmas. The dispersion relation of the IAWs is simply given by

$$\frac{\omega}{k} = c_s \tag{1.28}$$

being, ω k, the usual phase velocity of the wave. In weakly ionized plasmas, like the one considered here, the dominant damping mechanism of ion acoustic waves occurs through collisions with neutrals. The electron-neutral collision frequency can be estimated as follows

$$\nu_{e0} = v_{te} n_0 \sigma_0 \tag{1.29}$$

being, σ_0 the cross section of the electrons with the neutrals, which, for the case of an Argon gas, assuming an electron temperature of 1 eV, has a value around $2\times\ 10^{20} m^2$. The decay length δ of the wave, i.e. the distance the wave travels until its amplitude drops by a factor of 1/e which is also referred to as *damping length*, can be approximated by

$$\delta = \frac{2c_s}{\nu_{e0}} \tag{1.30}$$

1.8 The *fireball*

It is named *fireball* a phenomenon which appears when an electrode immersed in a plasma is polarized to positive voltage levels of the order of 100 V. In this case a plasma region forms, more emissive than the surrounding plasma, normally with spherical shape attached to the polarized electrode. The experimental investigation of such phenomenon showed that the plasma structure is made of a positively charged internal "nucleus", enriched by ions, surrounded by a double sheath structure, made of two shells of negative and positive charges, respectively. Such structure, whose dynamical equilibrium is given by the balance between the competing phenomenon of ion generation through ionization and ion losses due to the repulsive potential of the electrode, gives rise to a step-like potential profile, with potential drops of the order of the ionization potential of the used gas, and the associated electric fields.

The electric voltage-current characteristics of a *fireball* can become rather complex, with a hysteresis behaviour. Moreover, a *fireball* can exhibit oscillations, whose amplitude depends on the region of the characteristics explored, which ca be easily measured on the signal of the electric current collected, with typical frequencies of the order of few kHz.

1.9 A model for the VESPA experiment

Let us now define a simple model for a hot-cathode discharge, which will make use of the simple ideas given above [1]

The VESPA experiment, whose detail can be found in chapter 3, can be schematized as a system made of a cathode (the filament) emitting electrons and an anode, which is the vacumm vessel. Between the anode and the cathode a potential difference V is applied. In some sense, the system resembles the plane diode system, but with the difference that the anode surface is much larger than that of the cathode (we neglect, at this point, the effect of the permanent magnets). If the chamber is driven to high vacuum conditions, it is reasonable to expect a plane diode like behaviour,

[1] for a more complex and complete model, please refer to N. Jelic, S. Kuhn, R. Schrittwieser, Contrib. Plasma Phys. **43**, 94 (2003).

characterized by a current which initially grows with the applied voltage and then stabilizes at the value predicted by Richardson's law. The presence of a low-pressure gas in the chamber modifies such behaviour, as the electrons emitted by the cathode colliding with the gas atoms induce gas ionization (normally partial), thus producing a plasma. Such plasma will be characterized by a density n, an electron temperature T_e and by an electrostatic potential Φ. For the sake of simplicity, we will make the hypothesis that all these quantities do not depend on their position inside the chamber (which is normally true only far from the wall). The ion temperature will be much lower than the electron temperature, as the energy exchange between the two populations in these plasmas is not an efficient process. The approximation of null ion temperature is thus usually assumed. Around the cathode a Debye sheath will form, where potential fall between the plasma and the anode occurs. The electrons emitted by the cathode, also said primary electrons, will gain in this short length their energy, and the cathode will thus behave as an electron gun.

The model of the plasma is based in the balance between the charged particles produced by the ionization events from the primary electrons and the particles lost on the vacuum chamber, i.e. the anode (losses on the cathode are negligible, due to its small area).

The ionization cross section for Argon in the energy range of interest is given by the following formula:

$$\sigma_{ion}(E) = \theta \frac{(3e\Phi_I)^2(E - e\Phi_I)}{E(E + 8e\Phi_I)} \tag{1.31}$$

where E is the kinetic energy of the incoming electron, Φ_I is the Argon ionization potential (15.88 V) and θ is a constant equal to 2.90×10^{-21} m^2/eV. The mean free path for ionization is given by the expression

$$\lambda = \frac{1}{n_0 \sigma_{ion}} \tag{1.32}$$

where n_0 is the neutral gas atom density. The graph in fig. 1.8 shows the mean free path as a function of the gas pressure and the voltage difference between the cathode and the plasma (which, as will be shown later, is not very different from that applied between the anode and the cathode). It can be seen that for pressure lower than 10^{-3} mbar the mean free paths are larger than the dimension of the system: in this case the condition is said to be non-collisional. In such a regime, the ionization process occurs in the whole chamber volume; at larger pressure values the ionization preferably occurs close to the filament.

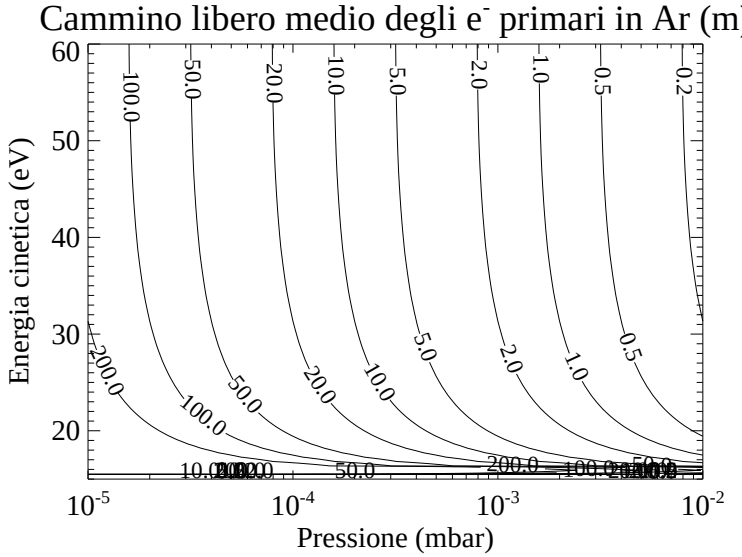

Figure 1.8: *Mean primary electron free path as a function of pressure and of thei energy.*

In the non-collisional limit, the mean number of ionization events induced by a primary electron will be $n_0 \sigma L_{eff}$, where L_{eff} is the length of the path followed by the electron in its motion inside

the plasma. The total number of ionization events per unit time is given by this quantity multiplied by the total flux of primary electrons, which is I/e, being I the discharge current flowing between the anode and the cathode. Such product, which represents the number of ions produced per unit time, must be equal to the total ion flux towards the walls. Using for the ion flux the expression found in the section dedicated to the Debye sheath, we get the balance equation

$$\frac{1}{2} n c_s A_i = n_0 \sigma L_{eff} \frac{I}{e} \tag{1.33}$$

where A_i represents the effective area hitted by the ion flux. Without magnets this will be the inner surface of the vacuum chamber. From this balance equation, the plasma density can be deduced

$$n = \frac{2 I n_0 \sigma}{e c_s} \frac{L_{eff}}{A_i}. \tag{1.34}$$

Fig.1.9 shows an example of plasma density values without magnets as a function of the discharge current and of the neutral gas pressure. An electron temperature of 2 eV has been considered and $L_{eff} = 20$ cm, which is the average distance between the filament and the vacuum chamber. Typical plasma densities are of the order of $10^{13} \div 10^{14}$ m^{-3}, which are rather low values(please compare to the values shown in fig.1.1). Nonetheless, the use of permanent magnets located on the vacuum chamber wall gives access to higher density regimes, as the edge magnetic fields (through a mirror effect) reflects and confine the particles approaching the wall itself. Therefore, the value of L_{eff} increases, while that of A_i decreases.

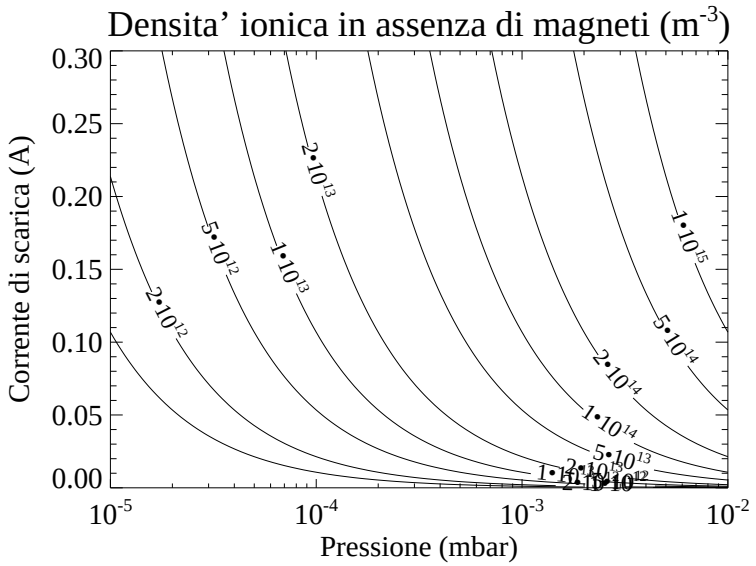

Figure 1.9: *plasma density estimated from ion balance, in the case without magnets.*

The plasma formation can occur for voltages between the filament and the chamber high enough to transfer to the electrons an energy sufficient for the ionization process of the Argon atoms (ionization potential:15.9 eV). By gradually increasing the voltage, low currents are at first measured, which correspond to the current emitted by the filament (typically in a range limited by space charge effects), possibly enlarged from ion contribution, associated to scattered ionization events (Townsend regime). When a given voltage is reached, named breakdown voltage, a rapid increase of the collected current is found, which corresponds to plasma formation. A strong variation is also observed of the electrostatic potential profile inside the chamber from that described by the plane diode model, characterized by a smooth variation of the potential from the filament to the wall, towards a situation with a potential fall occurring around the filament on the Debye sheath. In such a condition, the filament acts as an electron gun, emitting electrons having the energy given by the potential difference between the filament itself and the plasma, as they are accelerated on the short length of the Debye sheath.

CHAPTER 2

Elements of vacuum technology

2.1 Introduction to the problem

The creation of vacuum in the laboratory is an ancient problem, which has seen over the course of the years enormous progress. Today, it is possible to obtain pressures lower than 10^{-12} Pa in specific environments, such as parts of particle accelerators. The strong drive for improvement is due not only to purely scientific issues, but also to requirements coming from technological sectors, such as that concerned with thin film production and microelectronic devices.

Vacuum production implies the removal of gas or vapor molecules from a given container, and this requires a good knowledge of the gas behaviour, of the working principles of the devices used for vacuum production and measurement, and also of the behaviour of the structural materials in use.

2.2 Classification of vacuum levels

The term "vacuum" refers to the physical condition taking place in an enviroment where the gas pressure is lower than the atmospheric one. The measurement unit of pressure in the International System of units is the Pascal (Pa). In the experimental practice, though, it is frequent the use of other units, such as the millibar (mbar), equal to 100 Pa, and the mmHg, or Torr, equal to 133.3 Pa.

Depending on the pressure level, the phenomena that take place in a vacuum chamber can be different, and so are the means used to obtain and measure that pressure. Usually, different vacuum levels are defined, as shown in table 2.1.

Low vacuum	$10^5 \div 10^2$ Pa	$10^3 \div 1$ mbar
Medium vacuum	$10^2 \div 10^{-1}$ Pa	$1 \div 10^{-3}$ mbar
High vacuum	$10^{-1} \div 10^{-5}$ Pa	$10^{-3} \div 10^{-7}$ mbar
UHV	$< 10^{-5}$ Pa	$< 10^{-7}$ mbar

Table 2.1: *Pressure intervals of the different vacuum levels.*

In table 2.2 are shown the values of density (particles per unit volume) and mean free path for the different regimes, at the reference temperature of 22°C.

The classification of the vacuum levels is determined by the values of these parameters:

Low and medium vacuum: $10^3 \div 10^{-3}$ mbar

The mean free path is much smaller than the linear dimensions of the container (viscous flow regime). The gas density is very high. The number of molecules in the gas phase is much larger

Vacuum level	pressure (mbar)	n (m^{-3})	λ (m)
Low and medium vacuum	1013	$2.48 \cdot 10^{25}$	$6.5 \cdot 10^{-8}$
	1	$2.45 \cdot 10^{22}$	$6.6 \cdot 10^{-5}$
	10^{-3}	$2.45 \cdot 10^{19}$	$6.6 \cdot 10^{-2}$
High vacuum	10^{-5}	$2.45 \cdot 10^{17}$	6.6
	10^{-7}	$2.45 \cdot 10^{15}$	$6.6 \cdot 10^{2}$
UHV	10^{-9}	$2.45 \cdot 10^{13}$	$6.6 \cdot 10^{4}$

Table 2.2: *Density and mean free path for the different vacuum regimes.*

than that of the molecules deposited on the container walls. The pumping consists mainly in the removal of the molecules in the gas phase, and is not affected by the wall degassing.

High vacuum: $10^{-3} \div 10^{-7}$ mbar

The gas molecules are mostly on the walls, and the mean free path is larger than the container dimensions (molecular flow regime). The pumping consists in the removal of the molecules which detach from the walls and reach the pump individually, without interacting with other molecules.

UHV - Ultra high vacuum: $< 10^{-7}$ mbar

It is defined as the regime in which the time required for the formation of a single-molecule layer on the walls of the container is much larger than the time employed for the experiment or the process. In this way, it is possible to assume that a "clean" wall is available for all the required time. In this regime the residual molecules present in the container volume are directly extracted from the crystalline lattice of the wall material. This is the typical working condition in particle accelerators and fusion experiments, and is also the vacuum level reached in microprocessor production systems.

2.3 Vacuum production

A vacuum system consists of a vacuum chamber, where vacuum is formed, of pumping systems which extract the gas from the chamber, of the components required for operations to be performed in the chamber (e.g. valves, manipulators, etc.), of channels connecting the different parts, and of pressure measuring instruments.

The basic quantity related to a a vacuum system is the gas flow rate F, defined as the net quantity of gas flowing per unit time through a plane at constant temperature. In practice, it is expressed as $p(dV/dt)$, where p is the pressure measured on the reference plane and dV/dt is the volume change per unit time through the plane. F is thus proportional to the number of molecules crossing the plane per unit time: indeed, applying the perfect gas equation of state, it is possible to write $F = kT(dN/dt)$. The flow rate so defined has dimensions of pressure times volume divided by time, that is, in the International System, Pa m^3/s.

A gas flow takes place through a channel if a pressure difference is present between its ends. The channel ability to allow a gas flow is related to its geometric properties and to the state of the gas. In order to describe this ability, we introduce a quantity called *conductance*, defined as the ratio between the gas flow through the channel and the pressure difference at its ends, that is

$$C = \frac{F}{p_1 - p_2}. \tag{2.1}$$

The conductance is expressed, in the International System, in m^3/s. In practice it is often expressed in litres per second (L/s).

The inverse of the conductance is sometimes called, for obvious reasons, resistance or impedance. Indeed, there is a perfect analogy between potential difference, electric current and electric resistance on one side, and pressure difference, flow rate and 1/conductance on the other one. On the basis of this analogy, the conductance of several channels in parallel will be given by the sum of the

conductances, while in case of a series the reciprocal of the equivalent conductance will be equal to the sum of the reciprocals of the conductances.

The evacuation of a vacuum system is the operation by which gas molecules are expelled from the system, performed using a vacuum pump. This operation is called pumping. A figure of merit of a pump is its *pumping speed*. It is defined, for a pump which has the aspiration mouth at pressure p', as

$$S = \frac{F}{p'} \tag{2.2}$$

where F is the gas flow rate through the pump. Let us notice that the pumping speed has the same units as the conductance, that is m^3/s or L/s, even though it is conceptually different. If a pump with pumping speed S is connected to a vacuum system by means of a channel with conductance C, the effective pumping speed in the vacuum chamber (at pressure p) is different, and lower, than that of the pump alone (at pressure p'). The effective pumping speed S_e is computed, taking into account that the channel is in series with the pump, as

$$\frac{1}{S_e} = \frac{1}{S} + \frac{1}{C}. \tag{2.3}$$

It is therefore clear that using a pump with high pumping speed is useless if it is connected to the chamber through a channel with low conductance.

Apart from the gas initially present, there are several gas sources in a vacuum chamber, such as:

- leaks, that is small openings through which the external atmosphere can penetrate the chamber;
- degasing of the system walls, that is the passage into gas phase of molecules initially adhering to the wall surfaces;
- evaporation of substances or components present in the system to be evacuated;
- gas or vapours originating from the pump.

Taking into account these sources is required for a proper description of the pumping process. To a first approximation, it is possible to represent all these sources in a cumulative way through a flow rate F_0.

The pumping process can thus be described through a balance equation, where the change in the chamber pressure results from the pump effect and the sources described above. One has

$$-V\frac{dp}{dt} = Sp - F_0 \tag{2.4}$$

where p represents the pressure inside the chamber, V is the chamber volume and S is the effective pumping speed. The solution of this equation describes the time evolution of the pressure inside the chamber.

In the simplified case in which F_0 ed S are independent of the pressure, equation (2.4) can be analytically integrated, yielding

$$p(t) = (p_i - p_0)\exp\left(-\frac{S}{V}t\right) + p_0 \tag{2.5}$$

where p_i is the initial pressure at $t = 0$, and the *limit pressure*

$$p_0 = \frac{F_0}{S} \tag{2.6}$$

has been introduced. It can be seen that the pressure decreases exponentially, reaching asymptotically the limit pressure, which represents the best vacuum level achievable by the system. The limit pressure formula shows that, for a given pumping speed, the vacuum level can be improved by reducing F_0. This can be obtained eliminating leaks as much as possible and reducing degassing

through an accurate cleaning of the chamber and of all the objects inserted in it. This cleaning can be achieved mechanically and chemically, or through ultrasound cleaning and heating. It is also important to pay attention to the choice of the materials to be introduced in the vacuum chamber.

When a chamber where the limit pressure has been achieved is isolated from the pump, equation (2.4) has the solution

$$p(t) = p_0 + \frac{F_0}{V}t \tag{2.7}$$

(as long as S and F_0 remain constant). In this situation the pressure grows linearly with time, due to the effect of leaks and degasing.

2.4 Vacuum pumps

2.4.1 Introduction

The development of vacuum technology, from the first piston pumps to the great variety of pumps presently available, has been enormous. Nevertheless, the problem of reaching the most extreme vacuum levels, starting from atmospheric pressure, using a single pump is still unsolved. Indeed, each pump type has a specific pressure range in which it is effective. The best vacuum levels ar therefore achievable only through a combination of pumps.

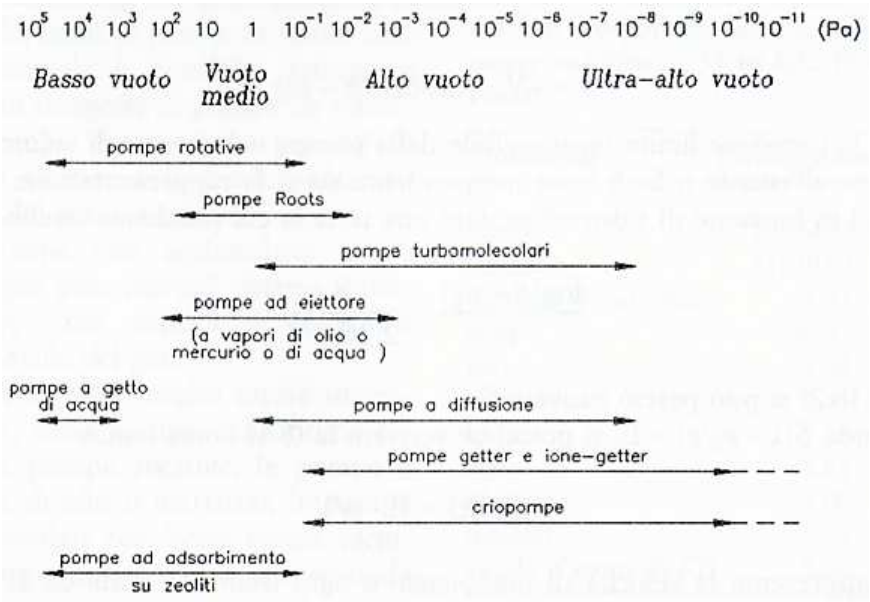

Figure 2.1: *Main types of vacuum pump and most common fields of use.*

Generally speaking, the pumps can be divided into two broad categories, that is those which remove gas from the system and transfer it to the outside and those which store it through appropriate methods of fixation of the molecules. Another classification can be made according to the specific working principle, according to the following scheme:

1. *mechanical pumps*, which require moving mechanical parts;
2. *pumps using a fluid*, in which the gas is removed through the action or the motion of a given fluid;
3. *getter pumps*, where the pumping effect is due to the chemical or physical adsorption of the gas or through ion capture;
4. *cryogenic pumps*, in which adsorption of the gas on surfaces at temperature equal or lower to that of liquid nitrogen takes place.

The main characterizing features of a pump are:

- pumping speed, as a function of pressure and of pumped gas;

- pressure range in which the pump is effective;
- pressure at the outlet;
- reachable limit pressure.

The pressure range in which the main pump types are effective are shown in figure 2.1; outside of those ranges the pumping speed decays very rapidly and the pump becomes ineffective. The reachable limit pressure depends on the losses from the pump, on the back-diffusion of the pumped gas, on the vapour pressure of the fluid eventually present in the pump and on the distance between the rotating parts and the stationary parts of the pump.

2.4.2 The rotary pump

The rotary pumps are the most used in the field of low and medium vacuum, and are frequently used to reach the pre-vacuum level for pumps which need to discharge the gas at pressures lower than atmospheric pressure.

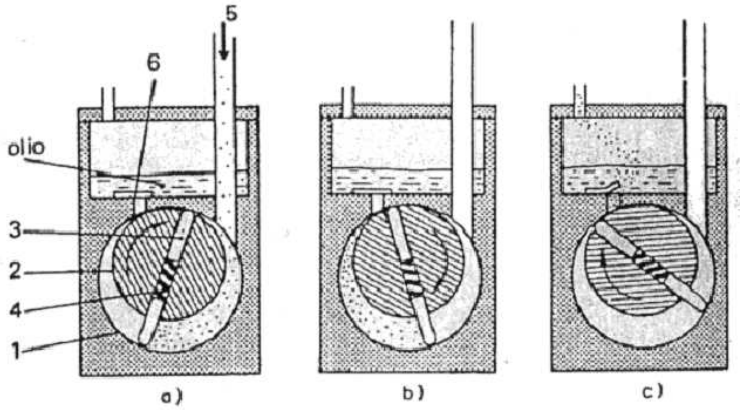

Figure 2.2: *Scheme of a rotary pump.*

As shown in figure 2.2, a rotary pump is made of a cylindrical body (1) inside which an eccentric rotor rotates in the direction marked by the arrow. In a groove on the rotor diameter are connected two vanes (3), which are pushed against the walls of the body by a spring (4). During the rotation, obtained through the action of an electric motor, these vanes compress the gas which enters through an opening (5) connected to the chamber to be evacuated, and then expel it through the outlet equipped with a valve (6). The outlet is immersed in oil, which has the multiple functions of sealing the outlet, of providing lubrification, and of assuring that the gas cannot escape through the contact point between the vane and the body surface, flowing from the region at high pressure to that at low pressure.

The compression ratio, that is the ratio between the pressure at the outlet and that at the inlet, which can be achieved by a rotary pump is of the order of 10^5, so that the minimum achievable pressure is of the order of 1 Pa, starting from atmospheric pressure.

The pumping speed of these pumps is generally almost constant from atmospheric pressure down to $(10 \div 1)$ Pa, and then has a rapid drop up to the limit pressure, which is around 10^{-1} Pa. Such behaviour of the pumping speed is shown in figure 2.3.

The presence of oil vapours or of its decomposition products in a vacuum system represents a negative issue, not only because it limits the pressure ultimately reachable, but also because hydrocarbons can have negative effects on the processes for which vacuum is produced. When rotary pumps are used in high vacuum systems, it is customary to equip them with devices for blocking oil vapours ("vapour traps"), which are for example made of a container full of alumina grains with a high effective surface. The traps can reduce the conductance between pump and chamber, and thus the effective pumping speed, when operating at pressures lower than 10 Pa. Special oils for rotary pumps have usually vapour pressure of around 10^{-3} Pa or lower, and are almost inert with respect to the main gases which are usually pumped in a vacuum system.

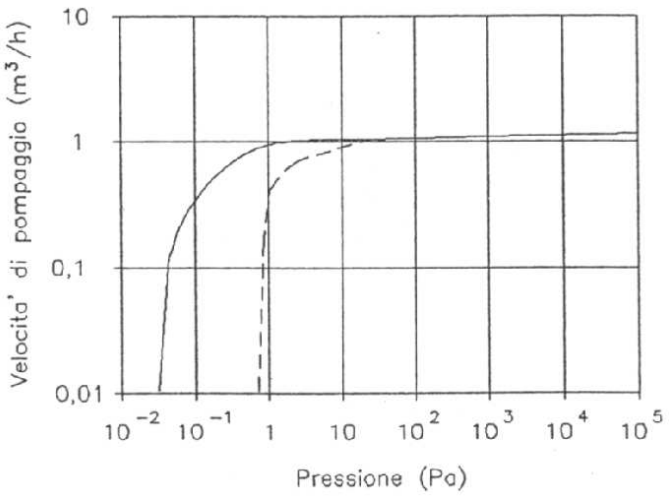

Figure 2.3: *Typical behaviour of the pumping speed of a rotary pump, as a function of pressure. — without gas ballast, – – with gas ballast.*

The gas ballast

Due to the high compression exerted on the gas by the rotary pump, it is possible that the gas liquefies if during the compression it reaches the critical pressure for vapour saturation at the temperature present in the pump (typically 60°C÷80°C). If, for example, a pump operating at a temperature of 70°C must pump water vapour, the compression could be such that the pressure becomes equal to 33320 Pa (saturated vapour pressure at 70°C); in this case, the water vapur will condense in droplets without being able to increase its pressure even more, and reach a value large enough ($\geq 10^5$ Pa) to open the discharge valve. The vapour thus remains in the pump in the form of liquid water, mixing with the oil and preventing the formation of a proper vacuum in the vacuum chamber; furthermore, the lubricant properties of the oil are degraded, and this can lead to a seizure of the pump.

To prevent this, a simple device called "gas ballast" is present in the pump. It is a valve which allows the insertion in the pump chamber, before the compression phase begins, of a precisely controlled quantity of air. This reduces the compression ratio, so that the extracted vapours are not able to condense. Clearly, the gas ballast reduces the pumping speed, as shown in figure 2.3. Thus, if the pump is connected to a system where the gas to be pumped contains small quantities of vapours (typicall water vapour in air), it is appropriate to activate the gas ballast when the pumping starts, in order to eliminate the vapours, and then close it after some time, allowing the pump t reach lower limit pressure. The working scheme of a rotary pump with gas ballast is shown in figure 2.4.

The rotary pump: advantages and disadvantages

Advantages:

1. can pump from atmospheric pressure, and thus can be used as pre-vacuum pump;
2. transfers the pumped gas to the outside, thus preventing problems of gas accumulation;
3. can be continously used also at high pressures;
4. robust and relatively cheap.

Disadvantages:

1. uses oil, with the risk of contaminating the vacuum system;
2. requires traps to block oil vapours;
3. relatively high limit pressure, of the order of $(1 \div 10^{-1})$ Pa;
4. possibility of oil degradation in presence of reactive gases.

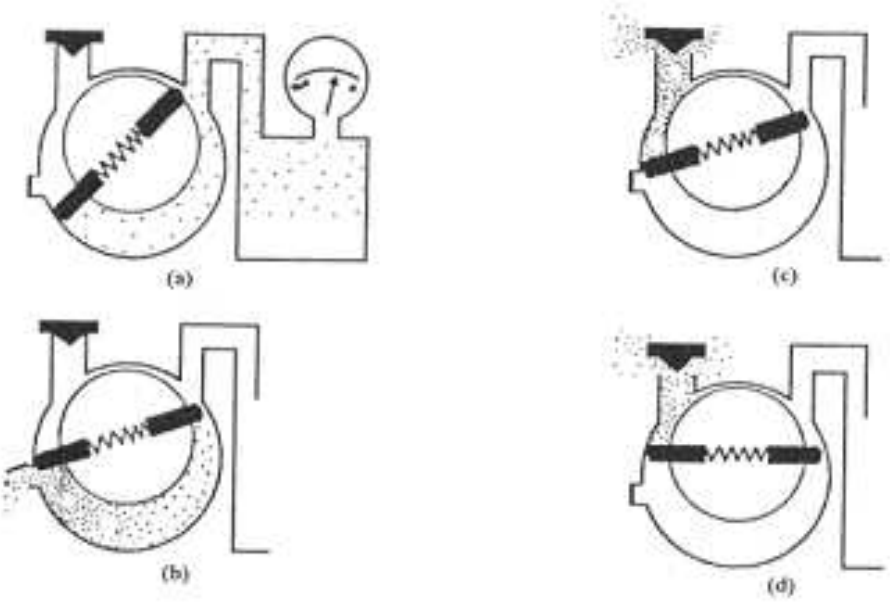

Figure 2.4: *Illustration of how a rotary pump with gas ballast works. a) the pump is connected with the chamber; b) the pump chamber is isolated from the main chamber; the gas ballast now opens, so that the compression chamber is filled with some fresh air which is mixed with the vapour; c) the discharge valve opens, and the particles of air and vapour are expelled; d) the pump continues the expulsion of air and vapour.*

2.4.3 The turbomolecular pump

Turbomolecular pumps are based on a principle known since 1913, according to which gas molecules hitting a surface in rapid movement, in a condition where collisions with walls are more frequent than those between particles (i.e. at low pressure), receive on average a momentum in the direction in which the surcae is moving, so that a gas flow in that direction is established.

As shown in figure 2.5, a turbomolecular pump consists of a stator and a rotor, with a shaft holding disks placed at small distance (typically around 1 mm) from other disks integral with the stator. The rotor turns at very high speed, around 70,000 turns per minute. The gas which penetrates the inlet is therefore "pulled" towards an outlet connected to a preliminary pump (typically a rotary pump) which expels it to the outer environment.

The compression ratio for this kind of pump is shown in figure 2.6.

The pumping speed is almost constant in a wide pressure range (from about 10^{-1} Pa to $10^{-6} \div 10^{-7}$ Pa for air). The typical behaviour of pumping speed with pressure is shown in figure 2.7.

The rotors of turbomolecular pumps are set in motion by motors directly connected to the shaft. The motor is powered by a "controller" at variable frequency, which controls the rotation velocity in the start up phase. Around one minute is required to bring small pumps from rest to full speed without current overload; big pumps may require several minutes. In order to achieve proper working conditions, the rotor must always be very precisely balanced. If the pump works for some time in an unbalanced situation, the bearings can overheat and be ruined. Other threats to the bearings are powders used in the system during the process or corrosive gases. Since the bearings are the most delicate component of a turbomolecular pump, pumps using magnetic levitation have been developed. These pumps do not require lubrification and operate at low temperature without the need of cooling.

The turbomolecular pump: advantages and disadvantages

Advantages:

1. transfers the pumped gas to the outside, thus preventing problems of gas accumulation;
2. absence of fluids, and therefore "clean" pumping;

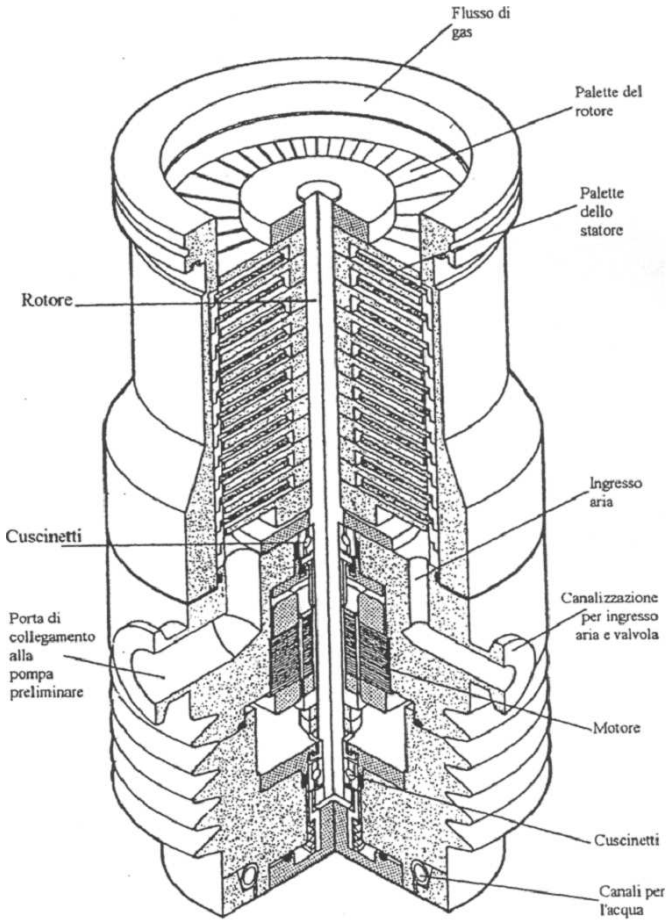

Figure 2.5: *Turbomolecular pump with vertical orientation.*

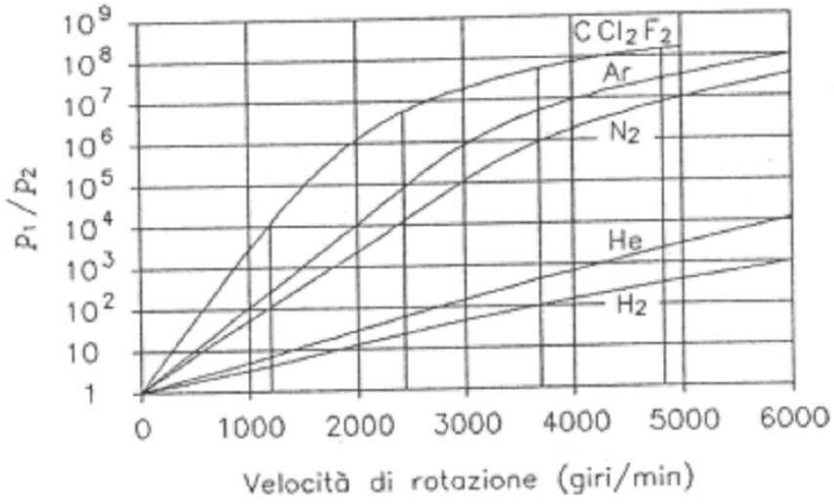

Figure 2.6: *Dependence of the compression ratio on the shaft rotation speed of a turbomolecular pump with a pressure of 10 Pa at the outlet.*

3. simple maintenance;
4. limit pressure of the order 10^{-8} Pa;
5. some pumps can be mounted with any orientation.

Disadvantages:

1. need of preliminary pumping up to (1÷0.1) Pa;

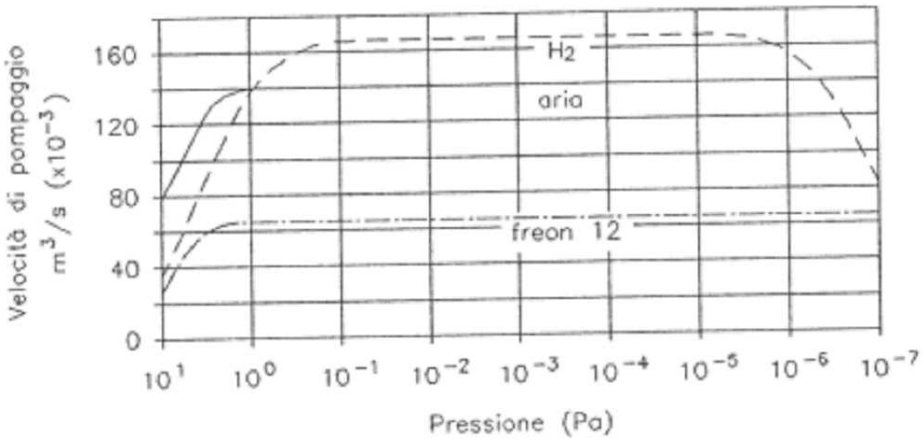

Figure 2.7: *Dependence of the pumping speed of a turbomolecular pump on the pressure for air, hydrogen and freon.*

2. reduced pumping speed for H_2;
3. delicate mechanical structure, especially for the largest pumps;
4. relatively high cost.

2.5 Vacuum joints

A vacuum system is generally made of different parts (chamber, pipes, pumps, etc.) which are connected by means of appropriate joints. The technology used for the joints depends on the desired vacuum level. In general, the joints are made thanks to flanges present on both parts to be connected. On the contact surface a gasket is placed to ensure vacuum tightness. For low vacuum systems the gaskets are made of organic materials, typically elastomers, while in UHV systems soft metals like copper or alluminum are used. In this latter case, the gaskets cannot be reused.

The standard flange systems used in vacuum technology are essentially three:

1. ISO-KF system
2. ISO-LF system
3. CF (or Conflat) system

There are also other systems with special gaskets for particular applications.

ISO-KF and ISO-LF standard flanges

Figure 2.8 shows an ISO-KF flange. It is used in low vacuum applications or for the connection between a high vacuum pump and a low vacuum one. The diameters of the pipes terminated by these flanges range between 10 mm and 50 mm. The gasket, also called o-ring, is made of elastomers. A commonly used material is VITON ®.

For high vacuum systems it is still possible to use ISO-KF flanges, provided that all parts and flanges are made of stainless steel and metal gaskets are used. This is because stainless steel is less porous and has less degassing than the aluminum used in low vacuum systems. The ISO-LF flanges are similar to the previous ones, but are used for largest pipes, with diameters from 63 mm to 400 mm.

CF (Conflat) flanges

Figure 2.9 shows the CF type flange, which is the standard system for high vacuum or UHV applications. While in the previous systems the flanges are held together by a vice, in this case screws are used. The material used for this kind of flange is stainless steel of standard grade 304 or

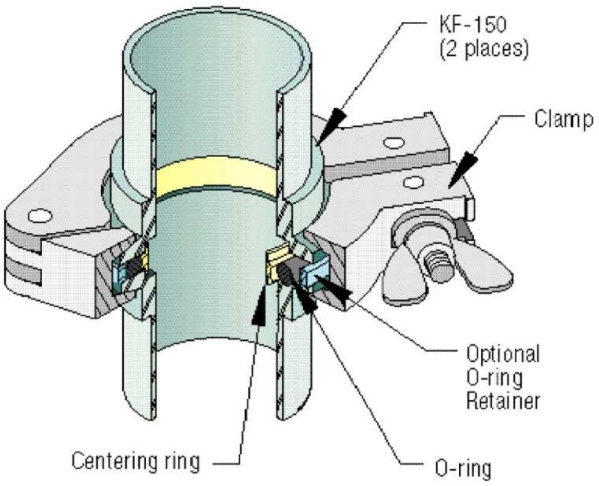

Figure 2.8: *Example of how two ISO-KF flanges are connected.*

316L. Other materials can be used in special applications. The standard gasket is made of copper, and this allows the use of this system at temperatures up to 400 °C.

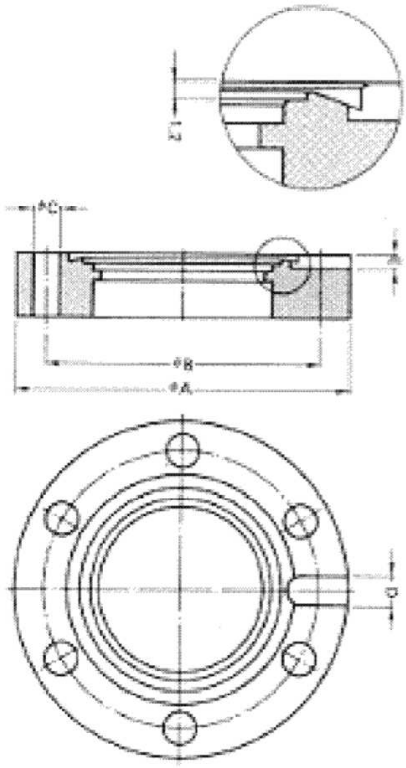

Figure 2.9: *CF flange.*

2.6 Vacuum measurements

The measurement of low pressures is a non trivial problem, especially when operating in the ultra-high vacuum regime. The pressure interval achievable in a vacuum system is so large (from 10^5 Pa to about 10^{-12} Pa) that it is not presently possible to have a single instrument type. Therefore, generally more than one instrument type will be present in the system, each covering a given pressure range.

The instruments used for vacuum measurements are called *gauges*. The main gauges fall into the following categories:

1. Mechanic gauges. The mechanic force exerted by the gas is used to change the level of a liquid column or to deform a thin sheet of material.
2. Thermal conductivity gauges. The thermal conductivity of the gas affects the heat loss rate of a heated element immersed in the gas.
3. Viscosity gauges. The gas viscosity is used to produce an aerodynamic resistance on a rotating body, or a damping of the oscillation amplitude of a suspended body.
4. Ionization gauges. The gas is ionized and the ion current reaching a collector is measured; in a partial pressure gauge the ions are separately collected according to their mass.
5. Discharge tube gauges. These are ionization gauges, but they use some features, like size or shape, of a gas electric discharge.

The different gauges cover different pressure ranges, as shown in figure 2.10.

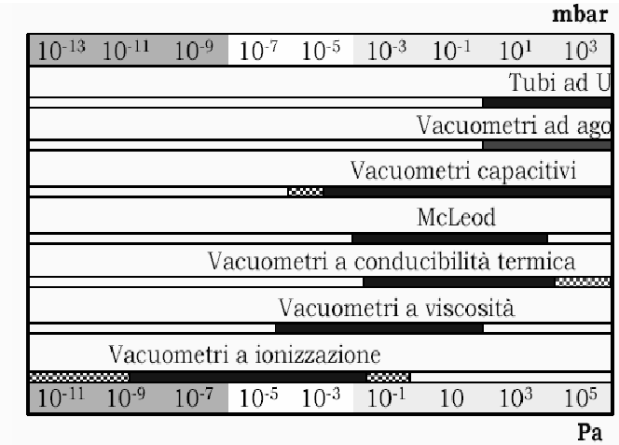

Figure 2.10: *Pressure ranges covered by the main types of pressure gauge.*

2.6.1 The Pirani gauge

The name of this instrument comes from M. Pirani, who described its basic working principle in 1906. It gives an indirect pressure measurement using the relationship between pressure and thermal conductivity or the gas. The working principle is the following: a metal filament with high temperature coefficient (tungsten or platinum) is placed axially in a cylinder of glass or metal connected to the vacuum system. When the filament is heated with a given electric power, the temperature that it reaches, and therefore its electric resistance, depends on the rate at which heat is dissipated through the gas. This, in turn, depends on the gas pressure if the mean free path of the gas molecules is larger than the box dimensions (in practice, for pressures less than about 2600 Pa). If the filament is inserted in a branch of a Wheatstone bridge, the resistance can be accurately measured, and this leads to the pressure value.

Since the Pirani gauge does not measure directly the gas pressure, but a physical quantity linked to it, a calibration is required. The calibration is different for each gas type. In general, the scale present on the instrument is calibrated for air. When operating with other gases, one should correct the measurement according to the calibration curves present in the instrument documentation.

2.6.2 The capacitive gauge

The capacitive gauge consists essentially in a metal body divided in two chambers by a thin diaphragm. One of the chambers is connected to the vacuum system, while the other is either connected to the external environment or is pumped to a pressure much lower than that to be

measured. In front of the diaphragm are placed one or two electrodes, which together with the diaphragm for an electric capacitor of given capacitance. This capacitor is inserted in a capacitive bridge, which is balanced if the pressure in the two chambers are equal, but becomes unbalanced when they are different. This happens because the diaphragm becomes curved and changes its distance from the electrode. The bridge unbalance is measured, and converted into a pressure measurement through a proper calibration. It is important to remark that this kind of gauge is very sensitive to temperature changes, which can produce changes in the diaphragm shape. It is therefore suggested to keep the instrument at constant temperature. In any case, it is important to wait that the gauge achieves thermal equilibrium before starting the measurement. The zero level must also be adjusted. The capacitive gauge is widely used for low and medium vacuum measurements, because it has the advantages of not having hot parts and filaments at high temperature, of not requiring electric or magnetic fields, and because it can be built with materials which are not damaged by reactive gases and vapours.

2.6.3 The ionization gauge

This gauge is made of three electrodes, that is a hot filament, a grid and a collector (or anode), mounted on a flange which allows to introduce them in the vacuum system. The electrons emitted by the filament are accelerated towards the grid by a potential difference V_g, generally in the range 70 V to 150 V. Many electrons, before hitting the grid, oscillate around it, as shown in figure 2.11, forming an electron cloud in the region between anode and grid. The ions produced by the collisions of these electrons with the gas molecules are accelerated towards the anode, called also ion collector, which is placed at a negative potential (for example -25 V) with respect to the filament, and is made by a thin wire oriented along the grid axis. The collected ion current yields the pressure, through a proper calibration.

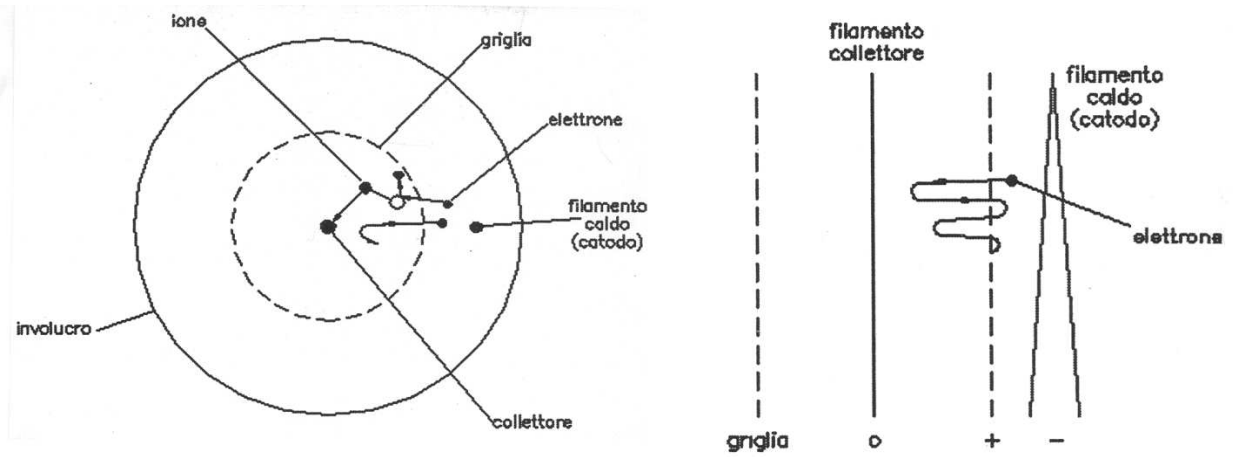

Figure 2.11: *Working principle of a Bayard-Alpert ionization gauge.*

This kind of instrument is simple, robust and appropriate for measuring pressures in the range from 10^{-1} Pa to 10^{-6} Pa. The upper limit is defined by the occurrence of electric discharges and space charge effects which cause a non-linearity of the relation linking ion current and pressure. The lower limit is due to soft X-rays produced by electrons hitting the grid. These X-rays, irradiating the collector, can extract secondary electrons from it. The secondary electron emission is not distinguishable from the arrival of positive ions, so that a term not dependent on pressure is introduced in the measurement. Indeed, the relationship between ion current and pressure loses its linearity around 10^{-6} Pa, and the curve becomes a line parallel to the pressure axis. In general, the measurement given by ionization gauges depends on the gas type, so that the measurement read on the instrument must be multiplied by an appropriate calibration coefficient.

CHAPTER 3

The VESPA experiment

This section is dedicated to a detailed description of the VESPA experiment. The set-up consists of a vacuum system, allowing to get a low pressure gas volume, of an electric part, which allows forming the plasma and performing Langmuir probe measurements and of a system of permanent magnets, located at the inner side of the vacuum wall, which can improve plasma confinement and hence increase plasma density.

3.1 The vacuum system

A scheme of the vacuum system is shown in fig. 3.1. It is made of the following main components:

- cylindric vacuum chamber (length: 80 cm, diameter 40 cm), divided into two halves by an electrostatically insulated grid;
- turbomolecular pump, with dedicated power supply;
- rotary pump for the establishment of pre-vacuum condition necessary for the turbomolecular pump;
- valve separating the chamber and the pumping system ;
- needle valve for gas puffing/filling with associated open/close valve;
- throttle (butterfly valve) for the turbomolecular pump ventilation, to be used during the switching off phases of the system;
- pre-vacuum measurement gauge (Pirani) and associated reading component;
- vacuum measurement gauge (ionization instrument, for vacuum measurement in the chamber) and associated reading component;
- capacitive instrument (baratron) for vacuum measurement during plasma discharge phases and associated reading component;
- alumina trap, to absorb oil vapors from the rotary pump.

The Vacuum chamber is equipped with various access ports. One of these ports connect the vacuum chamber itself with the rest of the vacuum system. Other ports are equipped with electric through, which electrically connect the inner and the outer regions of the chamber, maintaining the vacuum level. One these through systems is used for the Tungsten filament, while another one for some of the Langmuir probes installed in the chamber. A window is also installed for visual inspection of the chamber. Moreover, a manipulator is mounted on one side of the chamber, housing

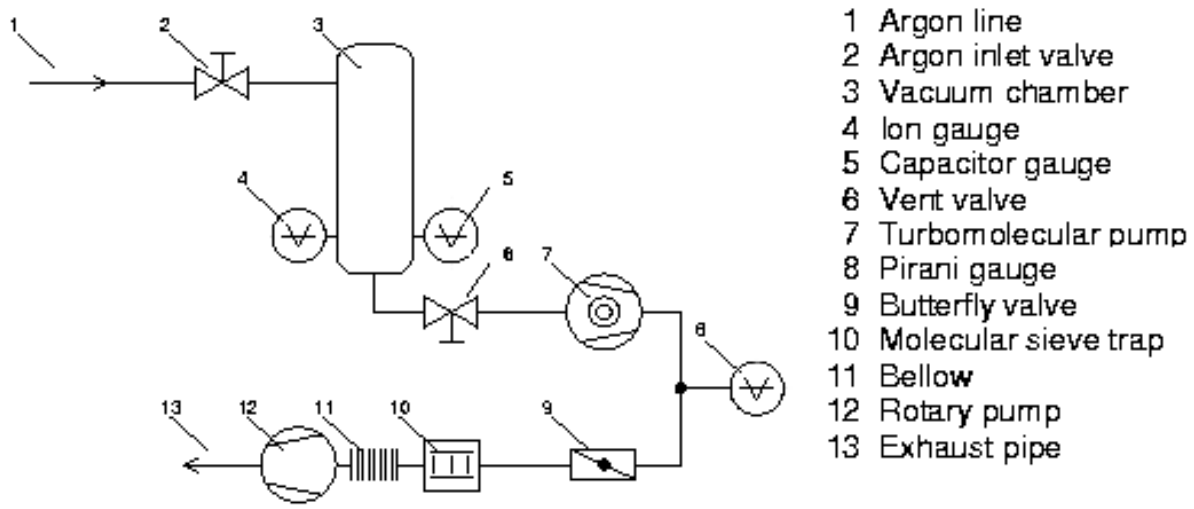

Figure 3.1: *Vacuum scheme of the VESPA experiment.*

six Langmuir probes distributed along the axis of the cylindrical chamber. The manipulator can be used to move such probe system, while maintaining the vacuum condition.

The vacuum, which is typically of the order of 10^{-5} mbar is obtained thanks to the use of the turbomulecular pump, with a typical rotation velocity of about 7000 turns/minute. The turbomolecular pump can operate only in the presence of a pre-vacuum system, condition produced by the rotary pump, which must drive the pressure down to values of about 10^{-1} mbar.

The rotary pump is equipped with a tap, driving the *gas ballast*. The gas ballast must be opened in order to introduce a small amount of atmospheric air in the pump chamber, with the aim of preventing the possible condensation of water vapor present in the gas to be pumped out and the subsequent oil contamination in the pump itself. The use of the gas ballast is particularly important when pumping a chamber which had been previously open to ambient air.

Even if it is not shown in the figure, an electrically controlled valve is installed in between the alumina filter. The aim of such a valve is insulate the rotary pump from the rest of the vacuum system, in order to prevent dangerous oil comebacks in the case of electric break-down.

The pre-vacuum level is measured by means of a **Pirani** instrument, whose sensitive part is located in between the rotary and the turbomolecular pumps. This diagnostics can measure pressure levels in the range from the atmospheric one and 10^{-3} torr, and it thus used to verify that the pre-vacuum gained condition is suitable for the use of the turbomolecular pump. On the Balzers instrument (named TPW 010) the measured pressure from the Pirani is visualized.

Tha vacuum obtained in the chamber is measured by means of a digital ionization gauge (Center One), suitable for the pressure range up to tra 10^{-7} mbar. It is worth to note that the indicated pressure must be multiplied by a calibration constant, which is 1 for air and 0.8 for Argon.

As the electrons emitted by the filament during the plasma formation phases could alter or even damage the ionization instrument. The instrument itself must be switched off during such phases. The pressure during the plasma phases will be measured by means of a capacitive instrument (**baratron**), which is less sensitive to charged particles than the ionization one, but more sensitive to thermal changes, so that it must be kept always switched on. The instrument installed in the VESPA experiment must be calibrated before each session. In particular, once the system has been driven to the lowest possible pressure, the value shown by the ionization instrument must be used as a reference to set the value on the baratron, by means of the screws C (course) and F (fine).

The valve between the chamber and the pumps is used to maintain some vacuum level even without active pumping. Such valve will be used to estimate the degassing properties of the

system, by measuring the characteristic time scale of the pressure growth once the chamber has been insulated.

The needle valve allows a fine tuning of the Argon gas filling the chamber, thus a good control of the operating pressure (which must be set to a predetermined stationary equilibrium). The needle valve is extremely sensitive and delicate, and the lower control knob must never be totally closed: to completely stop the gas inlet, the upper knob must instead be used (without using too much strength even in this case.

The throttle for the turbomolecular pump ventilation must be used when the pumps are switched off to let ambient air flow in the region between the turbomolecular pump and the rotary pump. The gas puffing has the effect of creating a high pressure region which impedes the comeback of oil form the rotary pump. The throttle must be opened gradually so that limited mechanical stress will be induced on the turbomolecular pump.

Finally, the **alumina trap** "traps" oil vapor which could comeback from the rotary pump.

The vacuum system is the most delicate part of the experiment, and must be handled with care and only after reading the associated instructions.

Everything, which, for any reason, will be installed inside the vacuum chamber, must be previously cleaned with care using alcohol or acetone. The use of gloves is recommended. Only the VITON o-ring can be handled with free hands as in this case the human grease is a good substitute to the normally used ones for vacuum systems.

The detailed operative instruction for the vacuum system (which will be also given to the students) must be carefully followed.

3.2 The electric scheme of the experiment

The electric scheme of the experiment, with the exception of that related to the Langmuir probe, is shown in figure 3.2.

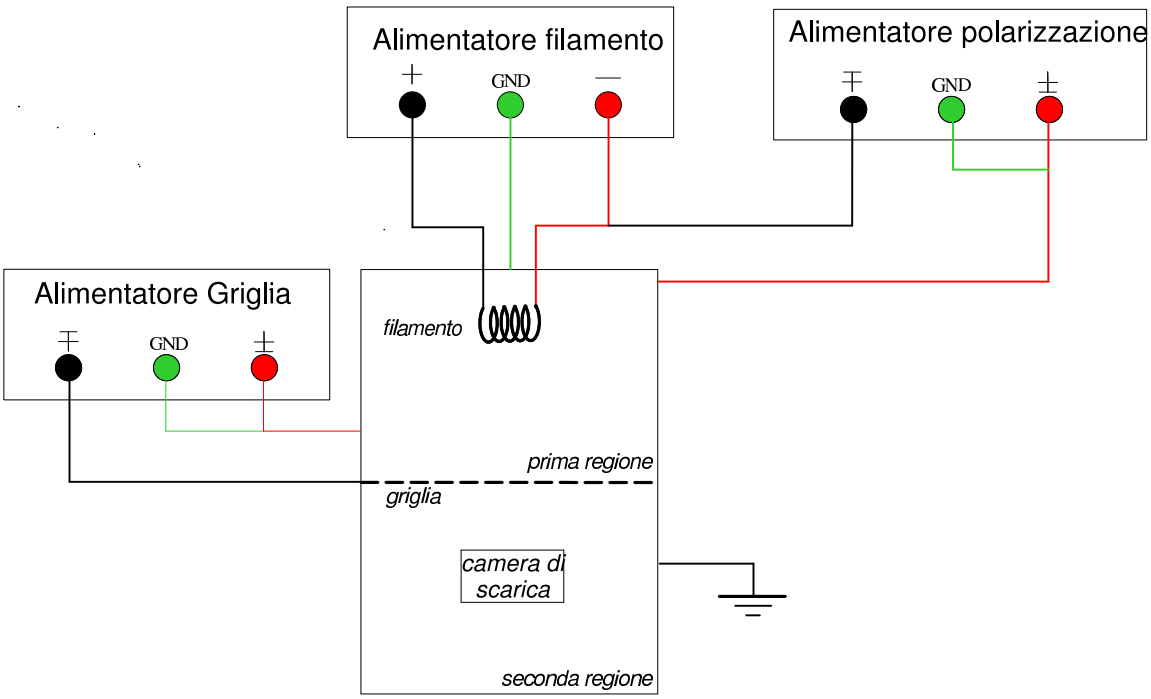

Figure 3.2: *Electric scheme of the VESPA experiment.*

The Isotech power supply, which has an output up to 36 V and 20 A, is used to drive the current in the filament, in order to heat it up to temperature values corresponding to significant emitted

electron currents. The current in the filament should never overcome 7 A, as the filament itself will be burnt.

The other Isotech power supply (IPS-603) can supply voltages up to 100 V and currents up to 3 A and is used for negative filament polarization with respect to the chamber electrically grounded. A plasma current is thus induced. A 1 Ω resistor can be mounted in series with the power supply (shunt resistor), located inside a white box, with the aim of precisely measuring the plasma current, through the measurement of the potential fall on the resistor.

A Kepco BOP 100-4M power supply, with outputs up to ±100 V and ±4 A, is used to polarize the grid dividing the two halves of the vacuum chamber. A 20 kHz polarization will be induced, by controlling the power supply with a waveform generator, in order to produce a density perturbation in the plasma and to excite a ion acustic wave (introduced in chapter 1). The propagation properties of such a wave will be investigated by using the Langmuir probes housed in the manipulator installed in the experiment.

3.3 The Langmuir probes

The VESPA experiment is equipped with three systems of Langmuir probes. One of these systems is installed in the manipulator, housing six probes made of Tungsten wires (1mm diameter) covered by a quartz tube, so that 1 cm long piece of Tungsten wire is exposed to the plasma. The probes are electrically connected to the outer part of the device through coaxial cables. The voltage to be applied to the probes is supplied by a four quadrants power supply (supplying positive/negative voltages and currents) Kepco BOP 100-1M, which has output values up to ±100 V e ±1 A. The power supply is remotely controlled by a PC, by means of a LabView interface, also used for data acquisition. The electric scheme for the Langmuir measurement is shown in figure 3.3.

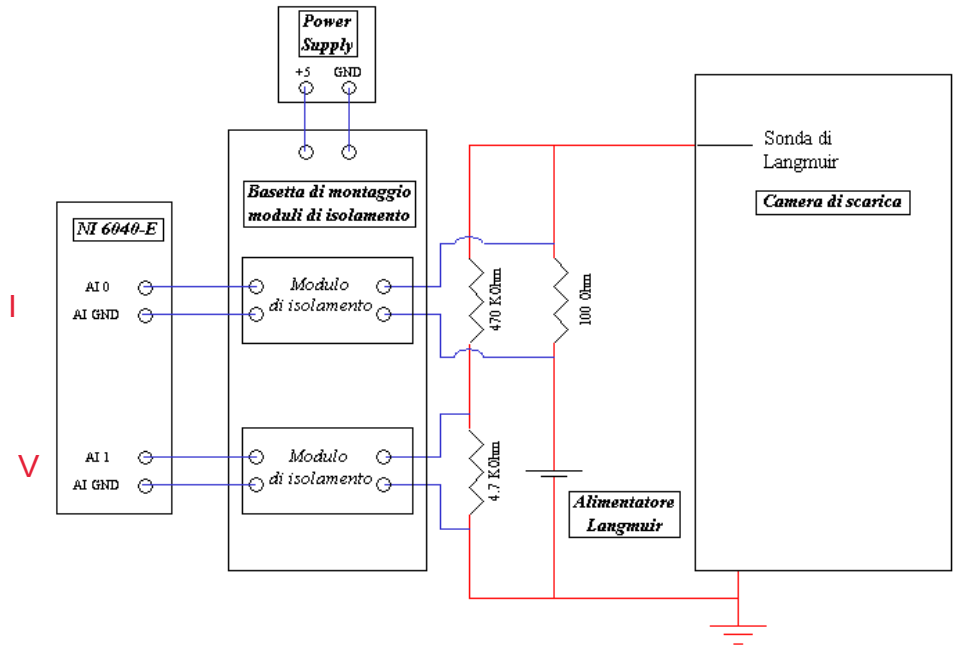

Figure 3.3: *Electric scheme for the Langmuir probe measurements.*

The voltage to the probe is measured through a resistive divider, made of two resistors 4.7 kΩ and 470 kΩ, respectively. The current collected by the probe is measured as the potential difference at the extremals of a 100 Ω resistor connected in series to the power supply. Both measures are obtained through an insulating module, necessary to protect the acquisition system itself, and

acquired by means of a National 6040-E Instrument board, housed in the PC.

Along with the use for the determination of the plasma parameters, the Langmuir probes mounted on the manipulator will be used to characterize the propagation properties of ion acoustic waves in the plasma. In particular, by driving these probes to the electron saturation regime, and hence measuring the fluctuations of the electron density, the phase shift, and hence the propagation velocity of the excited sinusoidal wave will be estimated. The measurement will be performed by means of the use an oscilloscope (Yokogawa) equipped with insulated input.

The probes can also be used to form and visualize the phenomenon of the *fireball* described in chapter 1, by polarizing the probe at rather large positive values in relatively high neutral gas pressure conditions.

3.4 The permanent magnets system

The inner side of the vacuum chamber is surrounded by two systems of permanent magnets, with the aim of confining the plasma, through a mirror effect, repelling charged particles flowing towards the walls.

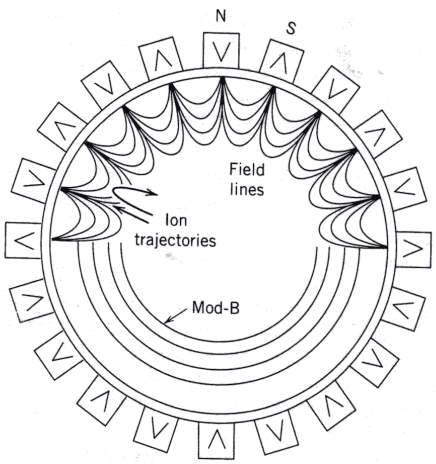

Figure 3.4: *Scheme of a section of the vacuum chamber from above, with the permanent magnets and the associated magnetic field lines. A typical ion trajectory, repelled by the magnetic mirror, is also indicated.*

The first set of magnets is made of two horizontal rows of magnets with the shape of parallelepiped, housed inside rectangular shape guides, forming a cage inside the chamber. The cage is interrupted where the lateral ports are located.

All the magnets of one horizontal row has the same polarity towards the inner part of the chamber. Adjacent rows have opposite polarity. A multipolar magnetic field is thus formed, as shown in figure3.4, where a schematic view of one chamber section seen from above is drawn. It is possible to show that the surfaces over which the magnetic field strength is constant are cylindrical surfaces, located at constant distance from the walls (few of these surfaces are indicated in the figure as Mod-B).

The second set of magnets is located on the two bases of the cylinder along parallel rows, with alternate polarity, and are directly exposed to the plasma.